Toxicology Letters 279 (2017) 125–135

Contents lists available at ScienceDirect

Toxicology Letters

journal homepage: www.elsevier.com/locate/toxlet

Refinement of the oral exposure description in the cyclic siloxane PBPK model for rats and humans: Implications for exposure assessment

Jerry L. Campbell Jr.[a,*], Melvin E. Andersen[b], Cynthia Van Landingham[c], Robinan Gentry[c], Elke Jensen[d], Jean Y. Domoradzki[d], Harvey J. Clewell III[b]

[a] Ramboll Environ, 6 Davis Drive, Research Triangle Park, NC 27709, United States
[b] ScitoVation, LLC, 6 Davis Drive, Research Triangle Park, NC 27709, United States
[c] Ramboll Environ, 3107 Armand St., Monroe, LA 71201, United States
[d] Dow Corning Corporation, 2200 W. Salzburg Road, Midland, MI 48686, United States

ARTICLE INFO

Keywords:
Cyclic volatile methyl siloxane
Octamethylcyclotetrasiloxane
Decamethylcyclopentasiloxane
D4
D5
Physiologically based pharmacokinetic model

ABSTRACT

The multi-compound, and multi-dose (MC-MD) route physiologically based pharmacokinetic (PBPK) model for cyclic siloxanes reported by McMullin et al. (2016) brought together the series of models for octamethylcyclotetrasiloxane (D_4) and decamethylcyclopentasiloxane (D_5) in rat and human into a unified code structure that would allow simulation of both compounds following the inhalation and dermal routes of exposure. The refined MC-MD PBPK model presented here expands upon this effort to include representation of rat kinetic data in plasma, tissues and exhaled breath for the parent compounds after oral bolus administration. Additional refinements were made with regards to hepatic induction of metabolism in the liver and allometric scaling of rate constants for the deep tissue compartments which will allow the MC-MD model to be used in uncertainty analysis. Overall, the refined MC-MD model was able to reproduce both parent D_4 and D_5 kinetic data in rat and human after inhalation exposure (rat and human) or dermal exposure (human). The inclusion of sequestered (i.e., lipid associated) oral absorption into plasma after oral bolus dosing successfully described the lack of exhalation as well as the initial distribution of siloxane to the liver which was higher than simple partitioning from plasma would allow. The refined MC-MD PBPK model presented here can be incorporated into uncertainty and variability analysis and cross-species dosimetry for both D_4 and D_5.

1. Introduction

Octamethylcyclotetrasiloxane (D_4) and decamethylcyclopentasiloxane (D_5) are low molecular weight cyclic volatile methyl siloxanes (cVMSs) primarily used in the production of high molecular weight silicone polymers. The use of D_4 as a direct ingredient in personal care products has declined significantly over the past 5 years. D_5 is still used as an intentional ingredient in cosmetics, consumer products and in dry cleaning. Persons who may be exposed include occupational exposure for workers, consumers and the general public and this will be predominately via low level inhalation or dermal exposures. To understand the influence of kinetic factors on delivered dose of these cVMSs, a comprehensive set of kinetic studies were conducted over the last several years. In association with development of these kinetic data, several PBPK models have been published describing the biological and physical-chemical processes regulating the kinetic disposition of either D_4 or D_5 in various species after different routes of exposure (Andersen et al., 2001; Reddy et al., 2003; Sarangapani et al., 2003; Reddy et al., 2007; Reddy et al., 2008). The individual models were each developed with specific data sets to describe the kinetic behavior of either D_4 or D_5 in rats or humans following various routes of administration. Recently, McMullin et al. (2016) combined the individual siloxane models into a single integrated multi-compound, and multi-dose (MC-MD) route PBPK model for cVMSs that provides a single code structure that can simulate D_4 or D_5 exposure in both rat and human allowing assessment of internal dose metrics in experimental animal and human for inhalation and dermal exposure.

The MC-MD model brought together the predominant exposure routes, inhalation and dermal, into a single code structure while maintaining the chemical specific characteristics that were similar as well as those that were unique due to the higher lipophilicity of D_5 (McMullin et al., 2016). These chemical specific characteristics include low blood:air partitioning, high fat:blood partitioning, high metabolic clearance by the liver, and slower loss from tissues than expected for simple well-mixed, flow-limited uptake compartments. The most notable characteristic was a discrepancy in the rate of exhalation given the

* Corresponding author at: Ramboll Environ, 6 Davis Drive, Suite 139, Research Triangle Park, NC 27709, United States.
E-mail address: jcampbell@ramboll.com (J.L. Campbell).

http://dx.doi.org/10.1016/j.toxlet.2017.04.002
Received 16 January 2017; Received in revised form 5 April 2017; Accepted 6 April 2017
Available online 11 April 2017

concentration in plasma, which indicated the presence of a pool of cVMSs in the plasma that was not available for exhalation. The inclusion of a blood lipid pool that was not available to be exhaled improved the model description of the amount of cVMSs available to be exhaled and several deep-tissue compartments to account for slow, multi-phasic loss from tissue after cessation of exposure.

Recent studies have provided plasma and tissue time-course data in adult male and female rats after oral bolus dosing with D_4 (30 mg/kg bw) or D_5 (100 mg/kg bw) administered in a rodent liquid diet (Domoradzki et al., 2017). The studies included measurement of both total radioactivity as well as parent (D_4 or D_5) in plasma, tissues, urine and feces along with measurement of the rate of amount in exhaled breath. An initial evaluation of the MC-MD model to describe the low dose oral data brought forth several deficiencies in the ability of the model to provide adequate prediction of the rate of amount in exhaled breath and time-course data for parent D_4 and D_5 in plasma, liver, fat, and exhaled breath. Notably, the rate of siloxane exhaled was significantly over-predicted, resulting in under prediction of the peak concentration in plasma and liver. The purpose of this study was to expand the oral absorption description in the MC-MD model to account for the initial uptake and distribution of D_4 and D_5 while restricting availability for exhalation.

2. Methods

2.1. Kinetic data

2.1.1. Rodent – inhalation studies

Single-exposure and multiple-exposure studies have been performed in which groups of 10 male and 10 female F344 rats were exposed by inhalation to 7, 70, or 700 ppm of D_4 (Plotzke et al., 2000a). In single-exposure studies, these animals were exposed to 14C-D_4 vapor for 6 h in a cylindrical flow-past, nose-only inhalation chamber following a conditioning period of 4 days. In multiple-exposure studies, after receiving the same conditioning, animals received a 6-h exposure of unlabelled D_4 for 14 consecutive days, followed by a 6-h exposure of 14C-D_4 vapor on the 15th day. Immediately after the last exposure, rats were placed in glass metabolism cages for collection of urine and feces and expired air. Excreta were collected at 6, 12, and 24 h and subsequently at each 24-h interval, up to 168 h post exposure. Expired volatiles were collected at 1, 2, 4, 6, 9, 12, and 24 h and subsequently at each 24-h interval, up to 168 h post exposure. In addition, plasma, perirenal fat, lung tissue, and liver tissue samples were processed for radioactivity measurements and chemical analysis of parent D_4 at similar time points (Varaprath et al., 1999, 2003). These data sets (Plotzke et al., 2000a) formed the basis of development of an inhalation PBPK model for D_4 (Andersen et al., 2001).

The PBPK model was further developed (Reddy et al., 2008) using data for the disposition of radiolabelled and parent D_5 in male and female Fischer 344 rats following single and multiple exposures at 7 and 160 ppm (Tobin et al., 2008). For the single-exposure, rats were exposed to 7 or 160 ppm 14C-D_5 vapor for six hours following 4 days chamber acclimation. For the repeat-exposure study, acclimated rats were exposed to 160 ppm unlabelled D_5 for 14 consecutive days and to 160 ppm 14C-D_5 on day 15. Immediately after the last exposure, rats were housed in glass metabolism cages for the collection of urine and feces at 6, 12 and 24 h and then at 24-h intervals up to 168 h. Expired volatiles were collected at 1, 2, 4, 6, 9, 12 and 24 h post exposure and at additional 24-h intervals up to 168 h. Air from the metabolism cages passed through an adsorbent for trapping volatiles and then through a CO_2 absorbent, allowing separate determination of the amount of $14CO_2$ and other volatile compounds, either parent D_5 or metabolites. Four or five rats per sex and dose were euthanized at the end of exposure and 1, 3, 12, 24, 48, 72, 96, 120 and 168 h post exposure and samples were collected including blood, perirenal fat, lungs and liver.

2.1.2. Rodent – oral studies

A detailed description of the oral studies can be found in this issue (Domoradzki et al., 2017). Briefly, adult male and female CDF (Fischer344)/CrlBr rats were administered a single oral bolus of 30 mg/kg D_4 or 100 mg/kg D_5. The dose was administered as radiolabeled compound to allow for measurement of both parent and total radioactivity (i.e., parent and metabolite).

2.1.3. Human datasets

Six male volunteers were exposed to 10 ppm of ^{14}C-D_4 as a vapor for 1 h while performing intermittent exercise (Utell et al., 1998). Total radioactivity was determined for blood, exhaled breath, and urine samples. Blood samples were collected during and after exposure up to 24 h post-exposure. Exhaled breath samples were collected up to 72 h after the cessation of the exposure. Three male and two female volunteers were exposed to D_5 vapor at 10 ppm for 1 h (Plotzke et al., 2002). During the exposure, subjects performed intermittent exercise, alternating rest and exercise periods on a regular interval. The corresponding changes in the ventilation rate and the minute volume were recorded. Blood and exhaled breath samples were collected during the exposure and the post-exposure period up to 24 h after the cessation of the exposure.

^{13}C-labeled D_4 (Plotzke et al., 2000a,b) or D_5 (Plotzke et al., 2002) was applied to the axillae of three male and three female subjects. A total of 1.4 g (males) or 1.0 g (females) was split equally between the two axillae. The material was allowed to absorb and evaporate for 5 min. Blood and exhaled air samples were collected over various time periods before and after the exposure.

2.1.4. Model structure

The MC-MD PBPK model for D_4 and D_5 is shown in Fig. 1. The model, which was reported by McMullin et al. (2016), incorporates the rodent and human PBPK models for inhalation and dermal as well as the additional compartments necessary to describe oral exposure into a single code structure. Physiological parameters (Table 1) such as ventilation rate (QPC, L/h/kg $BW^{0.75}$) and tissue blood flow rates (as percentage of cardiac output, L/h) were obtained from Brown et al. (1997). Chemical specific parameters are shown in Tables 2(D_4) and 3(D_5) for rat and human. As noted by McMullin et al. (2016), the MC-MD model is based on the D_5 inhalation model (Reddy et al., 2008) with modified parameter constants and compartments for D_4 using the Sarangapani et al. (2003) model. For D_5, all of the model features from the Reddy et al. (2008) inhalation model were retained with the exception of metabolism which was based on the saturable hepatic metabolism description from the Sarangapani et al. (2003) D_4 model. As will be discussed in detail below, the Sarangapani et al. (2003) model description in the MC-MD model had only been used for high inhalation concentration (700 ppm) repeated exposure and high dose oral bolus in the rat. For the current model, the hepatic metabolic induction is used for all simulations of D_4 and D_5. The MC-MD PBPK model (Fig. 1) has six tissue compartments including blood, fat, lung, liver, slowly perfused tissues, and rapidly perfused tissues. The deep compartment descriptions in blood and liver, the diffusion limited distribution to other tissue compartments and the mobile lipid pool descriptions were not impacted by the changes made to incorporate the oral bolus dose initial uptake and distribution description, which is described below.

2.1.5. Hepatic induction of metabolism

The previous MC-MD model had only incorporated metabolic induction in the liver for simulation of the high exposure 15 day study in rats based upon the Sarangapani D_4 model. For the revised MC-MD model presented here, induction is incorporated into all simulations for both rat and human whether it is a single or repeated exposure scenario. The Sarangapani description accounts for a delay in induction (i.e., a delay in response to allow production of enzyme) after exposure

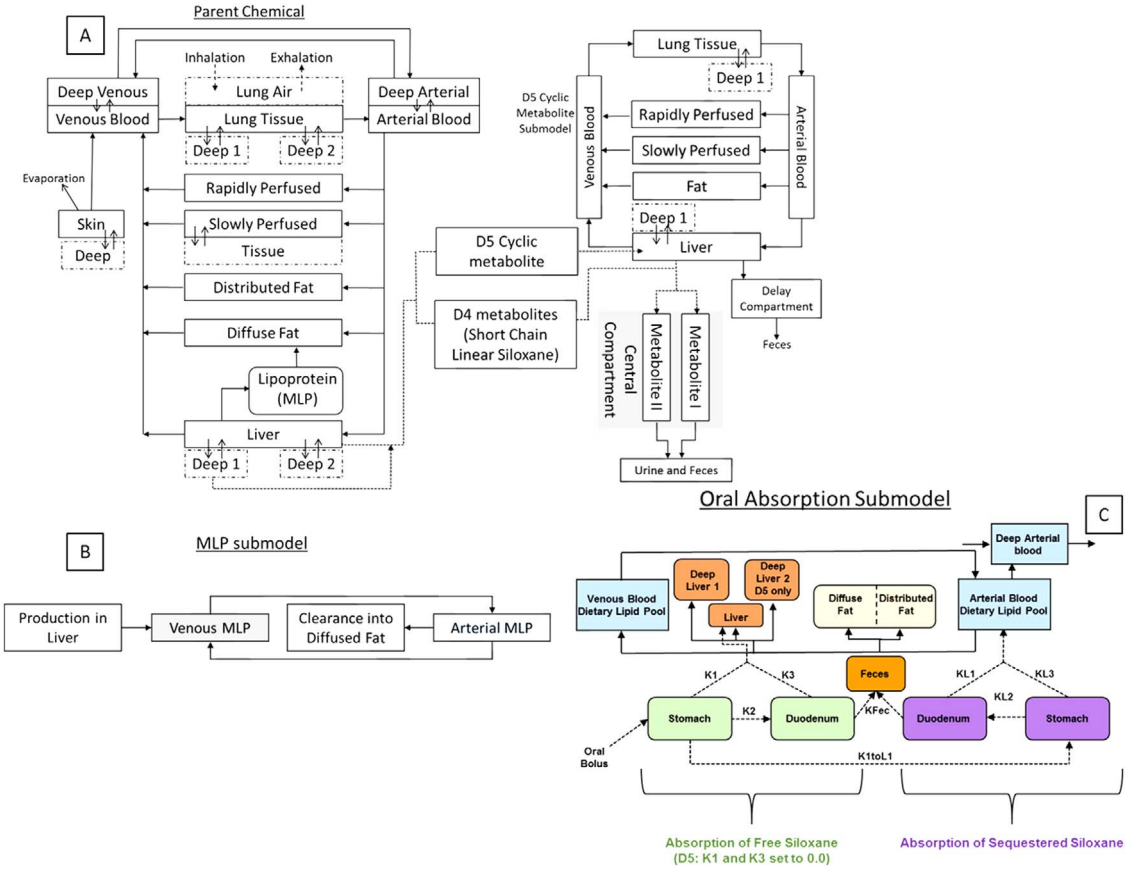

Fig. 1. MC-MD PBPK model schematic for D4 and D5 including the physiological model (A), the mobile lipid pool description (B) and the revised oral absorption sub-model (C).

Table 1
Physiological parameters used in the MC-MD model.

Physiological parameter[a]		Rat	Human
Tissue volumes (fraction of BW)			
Body weight (kg)	BW (kg)	0.185	70
Blood	VBLDc	0.074	0.079
Diffuse fat	VFATDIFFc	0.063	0.214
Distributed fat[c]	VFATDISTc	0.007	0.00
Liver	VLIVc	0.034	0.026
Lung	VLNGc	0.005	0.008
Rapidly perfused	VRAPc	0.100	0.080
Slowly perfused	VSLWc	0.627	0.437
Blood flows (fraction of QCC)			
Cardiac output	QCc [L/h/kg$^{0.75}$]	15	Varies[b]
Alveolar ventilation	QPc [L/h/kg$^{0.75}$]	15	15
Diffuse fat	QFATDIFFc	0.063	0.052
Distributed fat[c]	QFATDISTc	0.007	0.000
Liver	QLIVc	0.183	0.227
Rapidly perfused	QRAPc	0.411	0.472
Slowly perfused	QSLWc	0.336	0.249

[a] All physiological parameter values obtained from Brown et al. (1997).
[b] (−6.85 * log10(Age) + 16.8) * 60.0.
[c] Distributed fat turned off for humans.

to D_4 which reduces the impact of hepatic induction on a single exposure scenario. Upon cessation of exposure, the decay in induction (0.032/h) is set to the half-life of CYP enzyme. As noted above, hepatic induction had only been included in simulation of high exposure D_4 studies. McKim et al. (1998, 2001) provided experimental evidence that the induction as well as the increase in liver size relative to define first BW and hyperplasia in the liver resulted from D_4 having a phenobarbital-like effect on the rat liver. There is also experimental evidence that D_5 similarly affects the liver (McKim et al., 1999; Zhang et al., 2000); however, the impact of metabolic induction is less apparent as D_5 exposures have generally been lower than those of D_4 due to the lower volatility of D_5. In the model presented here, metabolic induction has been included in human simulations. The evidence available in the literature is that the cyclic siloxanes impart phenobarbital-like changes in the liver (McKim et al., 1999, 2001). As such, a similar change in liver would be expected for humans as has been shown in the rat. This change in the model will have essentially no impact on simulations of consumer and environmental exposure scenarios. The use of the model to evaluate human equivalent concentrations at a rodent derived point of departure may warrant human simulations at exposures that result in metabolic induction in the rodent.

2.1.6. Model parameterization

Several refinements to the MC-MD model parameterization as reported by McMullin et al. (2016) were undertaken in this effort. The primary focus was the expansion of the uptake and initial distribution of orally administered D_4 or D_5 driven by the recently collected oral kinetic data for parent compound reported by Domoradzki et al. (2017). The 1st order rate constants for deep tissue compartments in blood, liver and fat which had not been allometrically scaled in the previous iterations of the D_4/D_5 published models, were converted to clearances and scaled to the tissue volume. To accomplish this, the rate constants were divided by their respective tissue weights and then multiplied by the concentration in lieu of the rate constant times the amount (see Eq. (1)). The use of the total tissue volume for deep compartment parameter scaling was chosen because the tissue volume is readily identifiable compared to the actual mass of the deep tissue compartment, and the deep tissue compartment would most likely be represented in the model as a fraction of the tissue volume (e.g., fraction of tissue that was lipid). A notable result of the parameter scaling is that male and female rat kinetic time-course data for parent

Table 2
D_4 specific parameters for the cyclic siloxane MC-MD PBPK model.

Parameter	Label	Rat	Human
Partition coefficients (unitless)			
Blood:air	PBld	0.85	0.85
Diffuse fat:air	PFatDiffAir	100	100
Distributed fat:air	PFatDistAir	100	NA
Liver:air	PLivAir	21.2	21.2
Lung:air	PLngAir	7.84	7.84
Rapidly perfused:air	PRapAir	8.47	8.47
Slowly perfused:air	PSlwAir	8.47	8.47
Diffusion coefficients (unitless)			
Diffuse fat	PermFatDiff	0.4	0.4
Distributed fat	PermFatDist	0.3	NA
Slowly perfused	PermSlw	1	0.045
Metabolic parameters			
Maximal capacity (mg/h/$BW^{0.75}$)	Vmax	3.08	6.08
Affinity constant (mg/L)	Km	0.5	0.5
Induction of metabolism in liver			
Basal level of CYP (AUC/μg protein)	CYP0	15	15
Basal CYP production rate (AUC/h/μg protein)	K0	0.483	0.483
Basal CYP degradation rate (/h)	kElimCYP	0.0322	0.0322
Maximum CYP production rate (AUC/h/μg protein)	kMax	5	5
Dissociation constant CYP induction (μM)	kDLiv	0.67	0.67
Fraction returning from 1st deep liver compartment available for metabolism	FRLiDM	0.002	0.002
Mobile lipid pool (MLP) parameters (L/h, scaled to tissue volume)			
Production rate of MLP	KMLP	0.0408	3.78
Clearance from MLP compartment	Kremoval	0.055	0.39
Mass transfer parameters for deep compartments (L/h, scaled to tissue volume)			
Into deep arterial blood	kArtBldDeepIn	NA	NA
Out of deep arterial blood	kArtBldDeepOut	NA	NA
Into deep venous blood	kVenBldDeepIn	NA	NA
Out of deep venous blood	kVenBldDeepOut	NA	NA
Into 1st deep lung compartment	kLngDeep1In	0.018	0.018
Into 2nd deep lung compartment	kLngDeep2In	NA	NA
Out of 1st deep lung compartment	kLngDeep1Out	0.0166	0.0166
Out of 2nd deep lung compartment	kLngDeep2Out	NA	NA
Into 1st deep liver compartment	kLivDeep1In	0.5	0.5
Into 2nd deep liver compartment	kLivDeep2In	0.0012	0.0012
Out of 1st deep liver compartment	kLivDeep1Out	0.1	0.1
Out of 2nd deep liver compartment	kLivDeep2Out	0.007	0.007
Oral absorption rate constants (/h)			
Absorption rate 1st compartment	KABS	0.034	0.034
Transfer 1st to 2nd compartment	KABS2	0.1	0.1
Absorption rate 2nd compartment	K2ABS	0.17	0.17
Transfer from free to lipoprotein associated absorption	KORTOL	0.17	0.17
Absorption rate 1st lipoprotein associated compartment	KABSL	0.4	0.4
Transfer 1st to 2nd lipoprotein associated compartment	KABS2L	0.134	0.134
Absorption rate 2nd lipoprotein associated compartment	K2ABSL	0.067	0.067
Fecal excretion of unabsorbed oral dose	KFEC	0.15	0.15
Uptake into tissue from lipoprotein associated absorption (L/h, scaled to tissue volume)			
Into deep blood compartment from oral absorption lipid	KREMOVALBD	NA	NA
Into deep blood compartment from oral absorption lipid	KREMOVALF	0.5	0.5
Into distributed fat compartment from oral absorption lipid	KREMOVALFDIST	0.5	NA
Into liver compartment from oral absorption lipid	KREMOVALL	25	25
Fraction of liver compartment removal to 1st deep liver compartment	FRACOLDEEP1	0.4	0.4
Fraction of liver compartment removal to 2nd deep liver compartment	FRACOLDEEP2	0.0005	0.0005

Table 3
D_5 specific parameters for the cyclic siloxane MC-MD PBPK model.

Parameter	Label	Rat	Human
Partition coefficients (unitless)			
Blood:air	PBld	0.55	0.5
Diffuse fat:air	PFatDiffAir	1436	1436
Distributed fat:air	PFatDistAir	1436	NA
Liver:air	PLivAir	11.1	11.1
Lung:air	PLngAir	45.36	45.36
Rapidly perfused:air	PRapAir	3.4	3.4
Slowly perfuse:air	PSlwAir	7	7
Diffusion coefficients (unitless)			
Diffuse fat	PermFatDiff	0.026	0.026
Distributed fat	PermFatDist	0.02	NA
Slowly perfused	PermSlw	0.05	0.05
Metabolic parameters			
Maximal capacity	Vmax	30	11
Affinity constant	Km	20	10
Induction of metabolism in liver			
Basal level of CYP (AUC/μg protein)	CYP0	15	15
Basal CYP production rate (AUC/h/μg protein)	K0	0.483	0.483
Basal CYP degradation rate (/h)	kElimCYP	0.0322	0.0322
Maximum CYP production rate (AUC/h/μg protein)	kMax	5	5
Dissociation constant CYP induction (μM)	kDLiv	0.67	0.67
Fraction returning from 1st deep liver compartment available for metabolism	FRLiDM	0.002	0.002
Mobile lipid pool (MLP) parameters (L/h-kg tissue)			
Production rate of MLP	KMLP	4	3
Clearance from MLP compartment	Kremoval	2	1
Mass transfer parameters for deep compartments (L/h-kg tissue)			
Into deep arterial blood	kArtBldDeepIn	0.0016	0.0016
Out of deep arterial blood	kArtBldDeepOut	0.006	0.006
Into deep venous blood	kVenBldDeepIn	0.0016	0.0016
Out of deep venous blood	kVenBldDeepOut	0.006	0.006
Into 1st deep lung compartment	kLngDeep1In	0.6	4
Into 2nd deep lung compartment	kLngDeep2In	0.001	0.001
Out of 1st deep lung compartment	kLngDeep1Out	0.6	0.07
Out of 2nd deep lung compartment	kLngDeep2Out	0.007	0.007
Into 1st deep liver compartment	kLivDeep1In	0.5	0.5
Into 2nd deep liver compartment	kLivDeep2In	0.0012	0.0012
Out of 1st deep liver compartment	kLivDeep1Out	0.1	0.1
Out of 2nd deep liver compartment	kLivDeep2Out	0.007	0.007
Oral absorption rate constants (/h)			
Absorption rate 1st compartment	KABS	NA	NA
Transfer 1st to 2nd compartment	KABS2	NA	NA
Absorption rate 2nd compartment	K2ABS	NA	NA
Transfer from free to lipoprotein associated absorption	KORTOL	0.12	0.12
Absorption rate 1st lipoprotein associated Compartment	KABSL	0.08	0.08
Transfer 1st to 2nd lipoprotein associated compartment	KABS2L	0.46	0.46
Absorption rate 2nd lipoprotein associated compartment	K2ABSL	0.044	0.044
Fecal excretion of unabsorbed oral dose	KFEC	0.6	0.6
Uptake into tissue from lipoprotein associated absorption (L/h-kg tissue)			
Into deep blood compartment	KREMOVALBD	0.005	0.005
Into diffuse fat compartment	KREMOVALF	0.17	0.17
Into distributed fat compartment	KREMOVALFDIST	0.065	0.065
Into liver compartment	KREMOVALL	8.5	8.5
Fraction of liver compartment removal to 1st deep liver compartment	FRACOLDEEP1	0.8	0.8
Fraction of liver compartment removal to 2nd deep liver compartment	FRACOLDEEP2	0.0005	0.0005

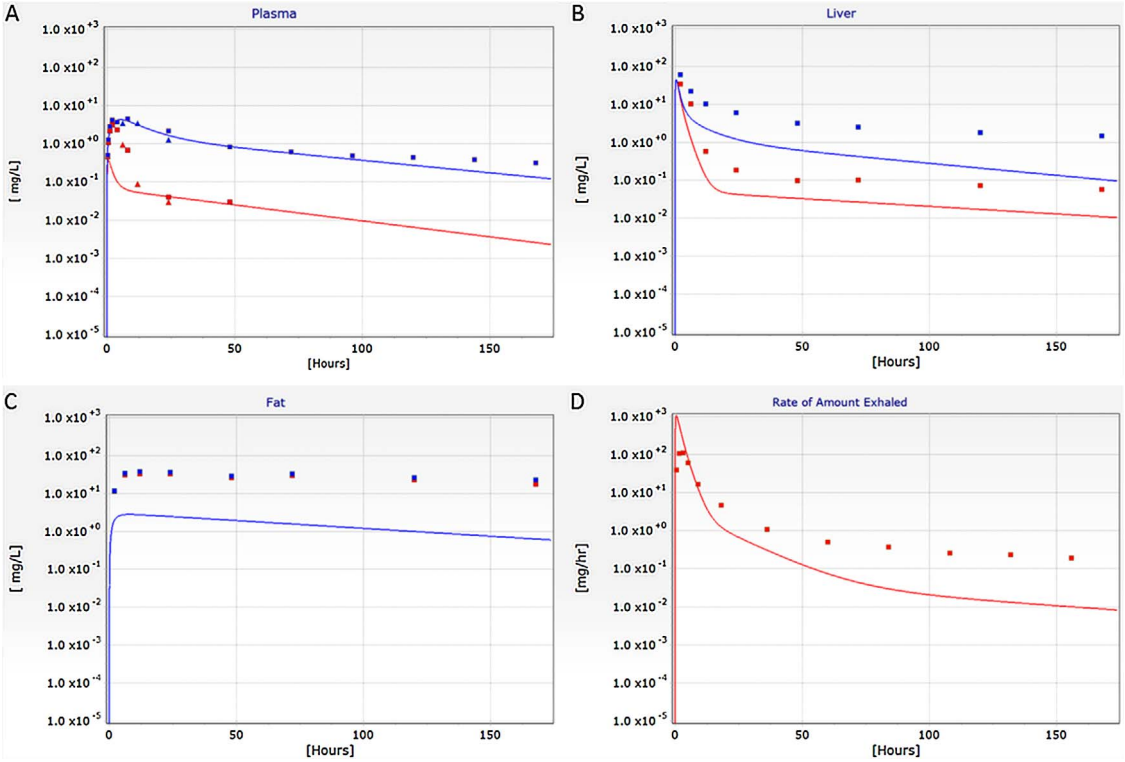

Fig. 2. Data (symbols) and model simulations (lines) of time-course concentrations of parent D4 in (A) plasma (B) liver (C) fat (D) rate of total amount of radiolabeled equivalents of D4 in exhaled breath (equivalent to parent D4 for exhaled breath) in male rats following a single oral exposure to 30 mg/kg administered in a liquid using the MC-MD model reported by McMullin et al. (2016). Red lines and data are parent D4 and blue lines and data are total radioactivity (Parent plus metabolite). (For interpretation of the references to color in this figure legend, the reader is referred to the web version of the article.)

compound can be described with a single set of parameters in lieu of the sex specific parameters required in the McMullin MC-MD model.

$$\frac{dA_{\text{deep}_i}}{dt} = \text{kIndeep}_i \times V_i \times C_i - \text{kOutdeep}_i \times V_i \times \text{Cdeep}_i \quad (1)$$

where the rate of change in D_4 or D_5 in the deep tissue compartment is the rate into the deep compartment (kInDeep_i) multiplied times the volume of the tissue (V_i) and the concentration of D_4 or D_5 in the tissue (C_i) and the rate out of the deep tissue compartment is the rate constant out of the deep compartment (kOutdeep_i) multiplied times the tissue volume (V_i) and the D_4 or D_5 concentration in the deep compartment (Cdeep_i) which is represented as the amount in deep_i divided by the tissue volume (V_i).

The oral time-course kinetic dataset reported in Domoradzki et al. (2017) showed that the majority of D_4 or D_5 absorbed orally was not immediately available for exhalation as evidenced by the simulated rate of amount exhaled overpredicting the measured rate of amount exhaled by greater than 10 fold for D_4 after a single oral bolus of 30 mg/kg (Fig. 2). The model failed to capture the peak parent concentration for D_4 or D_5 (data not shown) in plasma, liver or fat and measured parent concentration in liver was higher than partitioning from plasma compartment would entail. This would indicate that the cyclic siloxanes are absorbed in a sequestered form, possibly directly into plasma lipid or via chylomicrons. In order to account for this unique absorption profile, the oral uptake description in the model was expanded to allow both free and sequestered absorption with the primary distribution of the sequestered mass to the liver and fat compartments (Fig. 1c). The approach is similar to the efforts initiated by Dobrev et al. (2008) and expanded upon here as the addition of parent siloxane time-course data in plasma and tissues allowed the Dobrev construct to be refined to include the early distribution predominantly to the liver and fat. In the refined oral description, the siloxane mass orally administered is either taken up as free material using a pseudo 2-compartment gut description or transferred to and absorbed into plasma as part of the "dietary lipid" pool using a similar pseudo 2-comparment gut description. The mass absorbed in the latter pool is entered into arterial plasma bypassing the first pass in the liver as would be the case for absorption of free material directly from the GI tract. The 1st order rate constants from the GI tract (i.e., K1 and K1L) were scaled allometrically to $BW^{0.25}$. Uptake from this sequestered lipid pool in the arterial blood compartment into liver and fat is described as a clearance from the plasma pool into the tissue with the rate constant scaled to tissue volume (i.e., arterial plasma volume) as described above for the deep compartments. A portion of the lipid sequestered siloxane in the blood compartment if taken directly up into the deep liver compartment (D_4) or divided between the two deep compartments (D_5) to provide the best fit to time-course data in liver. In order to provide the best simulation of the D_5 oral kinetic data, a small portion of the sequestered uptake was taken into the deep plasma compartment. In the final analysis, the oral absorption of "free" cyclic siloxane is small when compared to the sequestered absorption for D_4 and was not included in the oral uptake of D_5 (i.e., K1C and K2C were set to zero).

Once the oral absorption rate constants had been established, it was noted that the use of free concentration in the liver did not provide a sufficient mass for metabolism (data not shown). A small fraction, 0.002 for D_4 and 0.007 for D_5, of the mass returning from the 1st deep compartment in the liver to the shallow liver compartment (i.e., blood exchange compartment) was included in the rate of change in the amount of siloxane metabolized. The assumption is that the release of this mass from the 1st deep compartment is directly to the liver tissue compartment and may be co-localized with the metabolic enzymes where it would have "special access" to being metabolized not necessarily reflected by calculation of "free" concentration based solely on the tissue:blood partition coefficient.

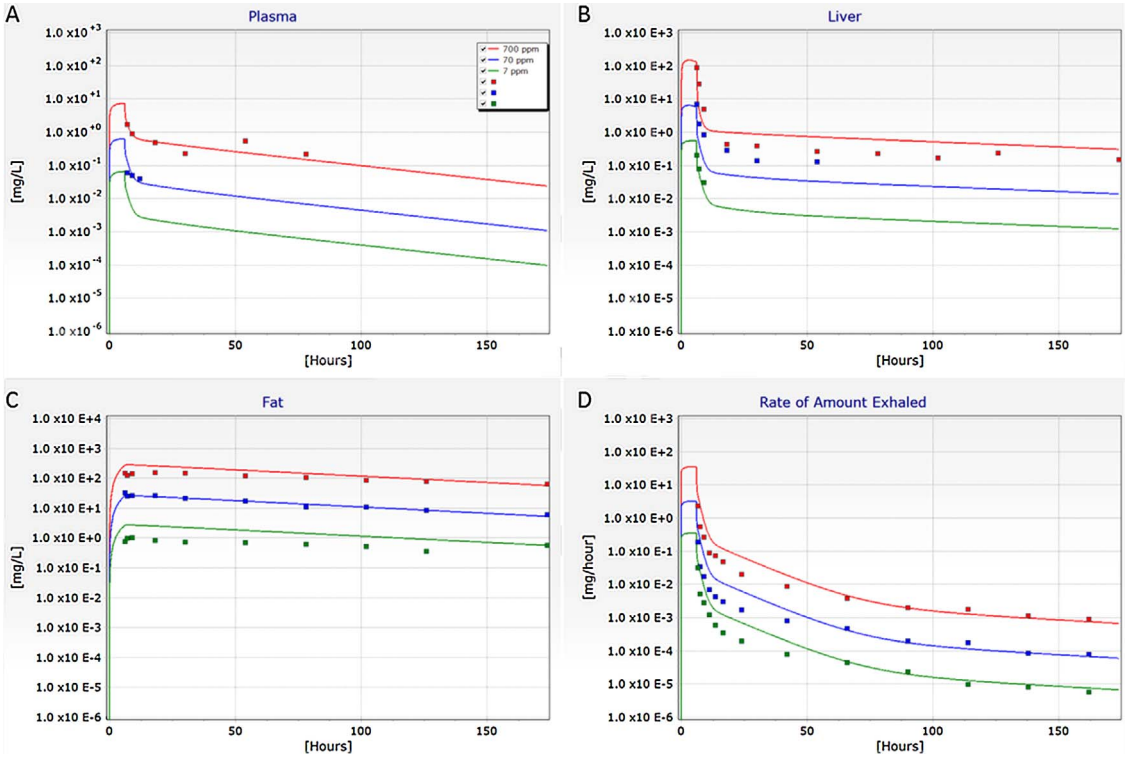

Fig. 3. Data (symbols) and model simulations (lines) of time-course concentrations of parent D4 in (A) plasma (B) liver (C) fat (D) rate of total amount of radiolabeled equivalents of D4 in exhaled breath (equivalent to parent D4 for exhaled breath) in male rats following a single 6-h inhalation exposure to 700, 70 or 7 ppm D4.

3. Results

Simulation of the D_4 and D_5 inhalation studies in rats (single and repeated doses) are shown in Figs. 3–6. The refinements to the MC-MD model did not impact the good agreement with the measured parent D_4 or D_5 in plasma, liver, fat or rate of amount exhaled following inhalation exposure as was presented by McMullin et al. (2016). The model provided excellent agreement with the measured tissue concentrations with nearly all data predicted within a factor of two. As with the McMullin MC-MD model, the revised model maintains the tendency

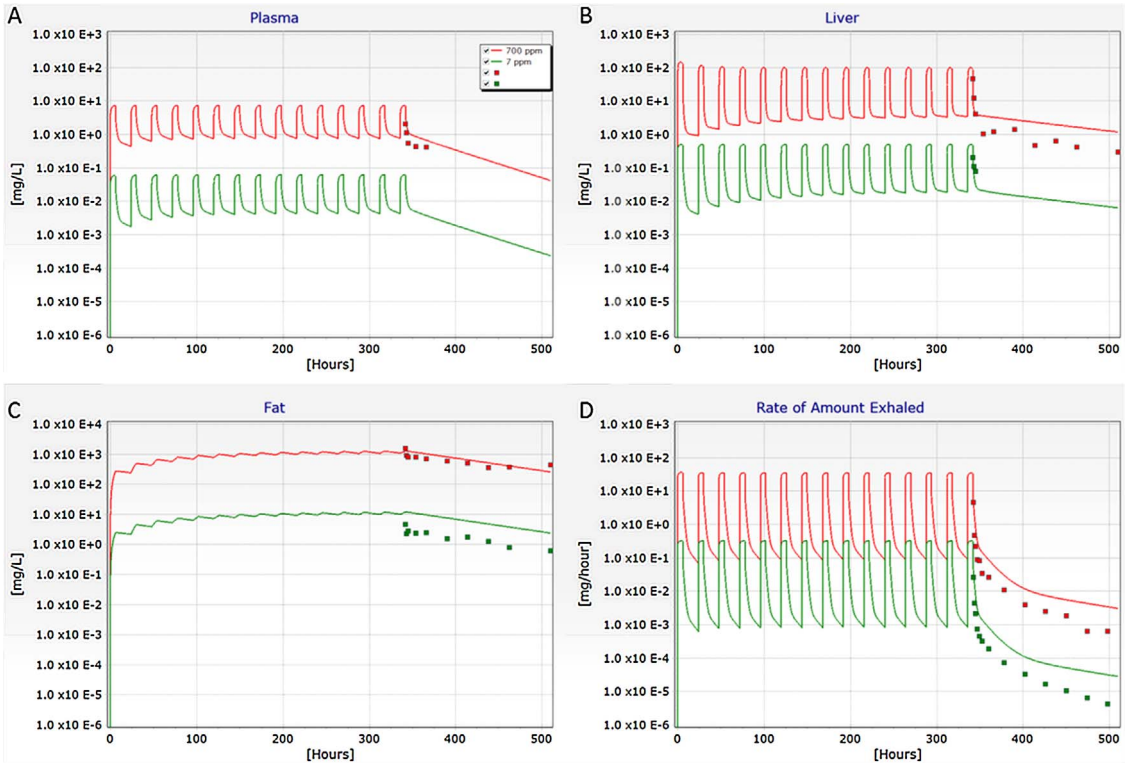

Fig. 4. Data (symbols) and model simulations (lines) of time-course concentrations of parent D4 in (A) plasma (B) liver (C) fat (D) rate of total amount of radiolabeled equivalents of D4 in exhaled breath (equivalent to parent D4 for exhaled breath) in male rats following a 15 daily 6-h inhalation exposures of male rats to 700 or 7 ppm D4.

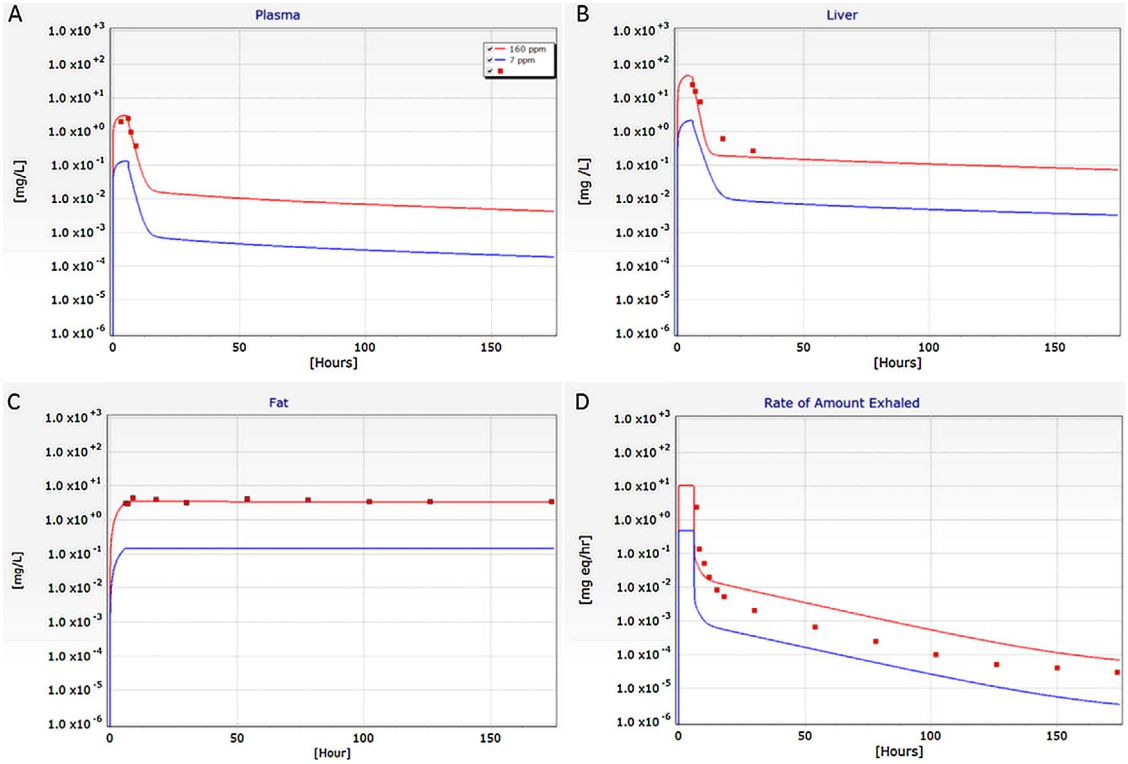

Fig. 5. Data (symbols) and model simulations (lines) of time-course concentrations of parent D5 in (A) plasma (B) liver (C) fat (D) rate of total amount of radiolabeled equivalents of D5 in exhaled breath (equivalent to parent D5 for exhaled breath) in male rats following a single 6-h inhalation exposure of male rats to 160 or 7 ppm D5.

to overpredict the terminal phase rate of amount exhaled, albeit within a factor of 3 of all of the data and a factor of 2 for most of the data. This is not entirely surprising as the mass exhaled after the first 36 h post exposure is small, represents a small fraction of the total mass of cyclic siloxane exhaled, and would not be expected to influence tissue based dose metrics given the very good agreement with the available tissue and plasma data.

The expansion of the simple pseudo physiological two compartment description of oral absorption used in the previous models to include a mechanism for sequestered absorption, provided excellent agreement

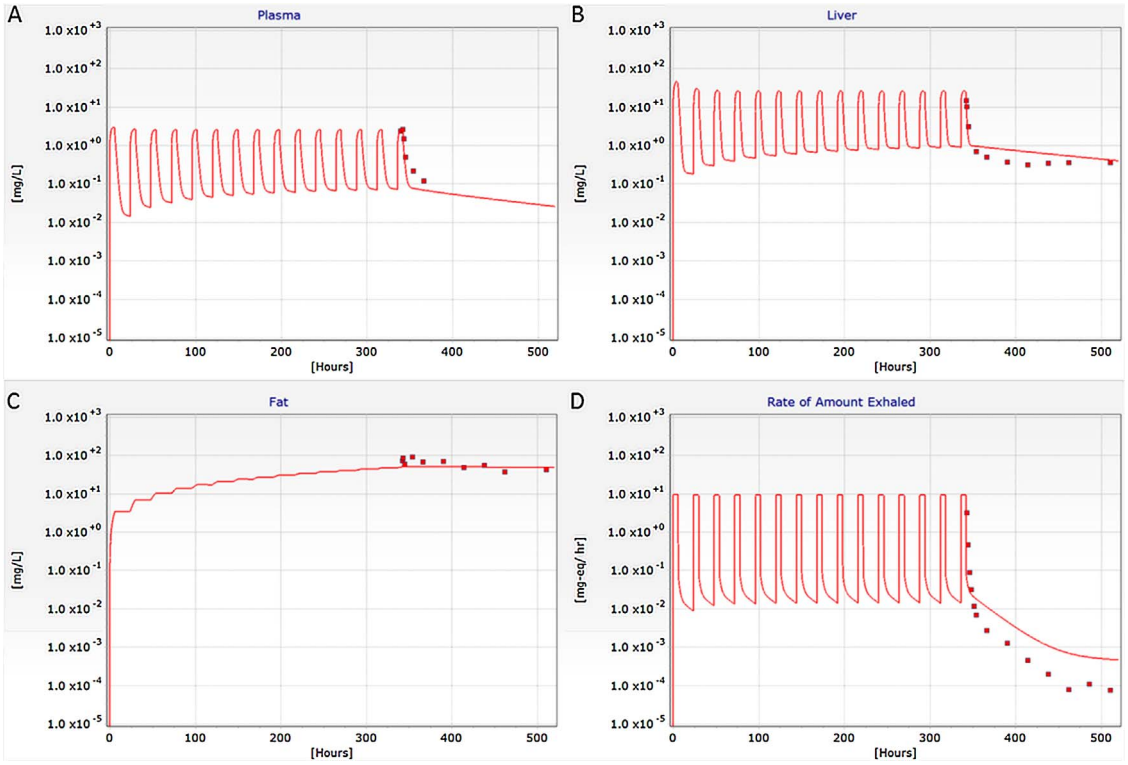

Fig. 6. Data (symbols) and model simulations (lines) of time-course concentrations of parent D5 in (A) plasma (B) liver (C) fat (D) rate of total amount of radiolabeled equivalents of D5 in exhaled breath (equivalent to parent D5 for exhaled breath) in male rats following a 15 daily 6-h inhalation exposures of male rats to 160 ppm D5.

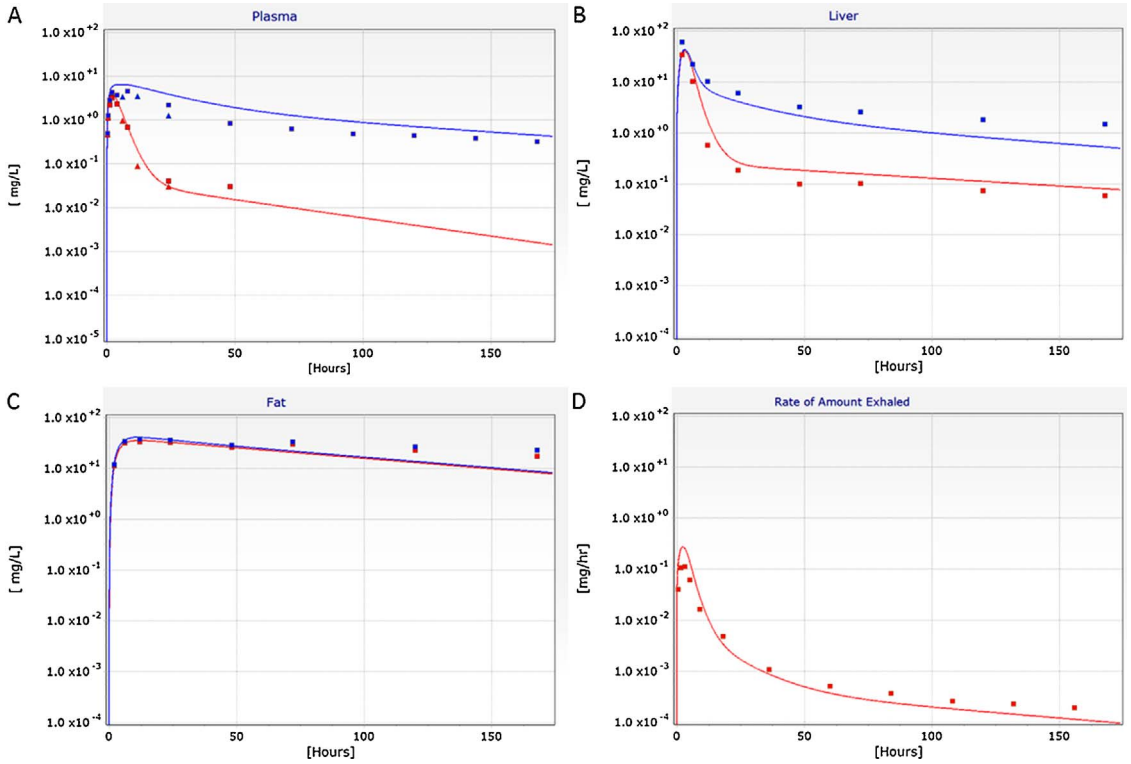

Fig. 7. Data (symbols) and model simulations (lines) of time-course concentrations of parent D4 in (A) plasma (B) liver (C) fat (D) rate of total amount of radiolabeled equivalents of D4 in exhaled breath (equivalent to parent D4 for exhaled breath) in male rats following a single oral exposure to 30 mg/kg administered in a liquid. Red lines and data are parent D4 and blue lines and data are total radioactivity (Parent plus metabolite). (For interpretation of the references to color in this figure legend, the reader is referred to the web version of the article.)

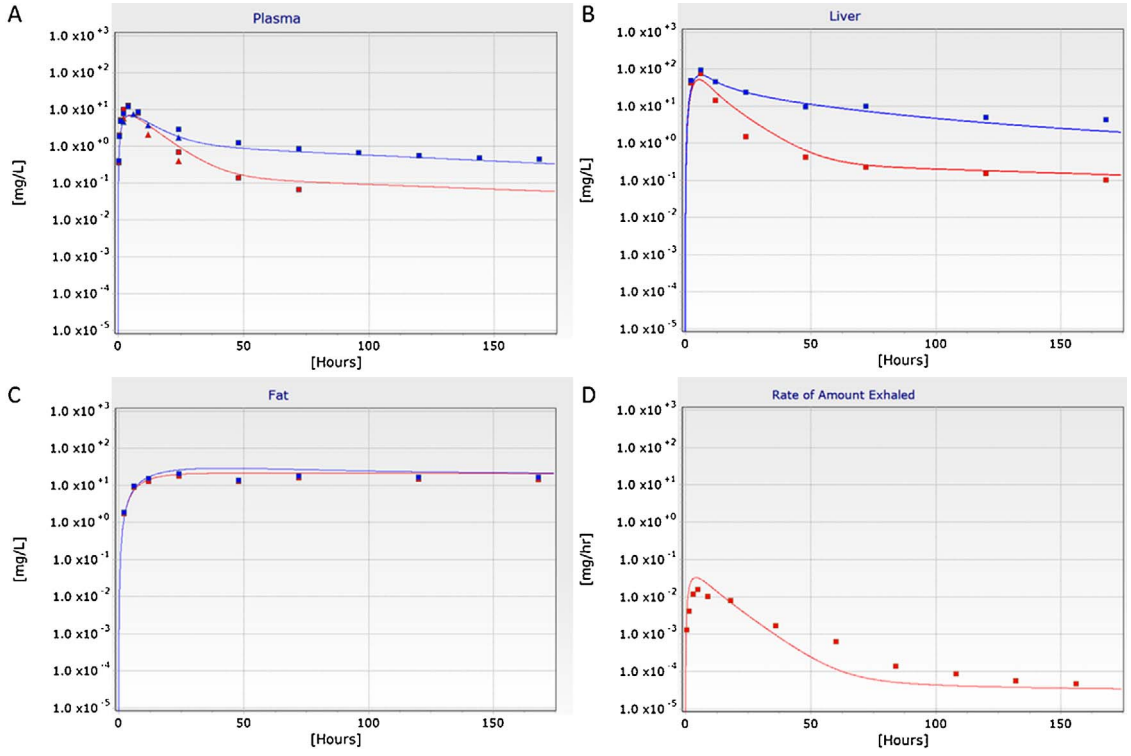

Fig. 8. Data (symbols) and model simulations (lines) of time-course concentrations of parent D_5 in (A) plasma (B) liver (C) fat (D) rate of total amount of radiolabeled equivalents of D_5 in exhaled breath (equivalent to parent D_5 for exhaled breath) in male rats following a single oral exposure to 30 mg/kg D_5 administered in a liquid. Red lines and data are parent D_5 and blue lines and data are total radioactivity (Parent plus metabolite). (For interpretation of the references to color in this figure legend, the reader is referred to the web version of the article.)

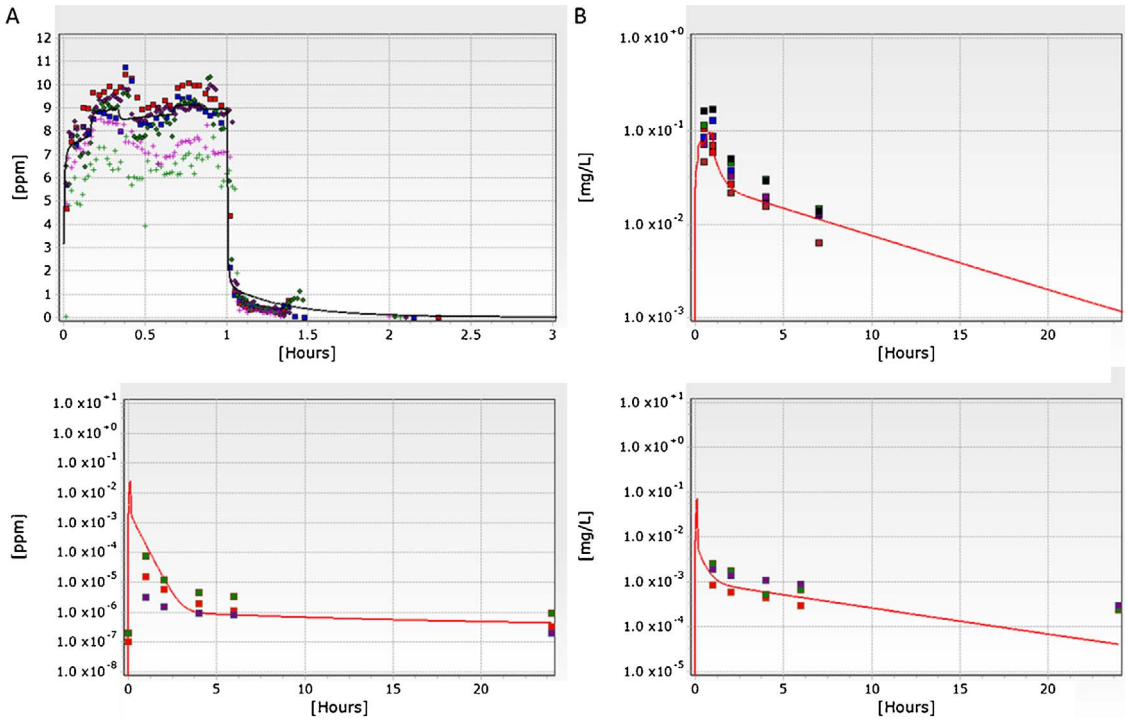

Fig. 9. Model simulation (lines) and data (symbols) (mean ± SD; $n = 5$) of D4 in (A) exhaled breath and (B) plasma in male human volunteers during and following 10 ppm D5 vapor exposure for 1-h or (C) exhaled breath and (D) plasma during and following a single application of 1.4 g 13C-D4 to skin axilla.

with the lower dose oral data for D_4 (Fig. 7). As compared to the MC-MD description (Fig. 2) where the peak rate of D_4 exhaled was overpredicted by a factor of 10, the revised description provided extremely good agreement with both the parent (red lines and data) and total radioactivity (blue lines and data) with all data falling within a factor of 2 of the model simulation. Initially, the D_4 oral absorption parameterization was used to simulate D_5 oral absorption. As was seen with simulation of D_4 oral kinetics using the McMullin MC-MD model for D_4, the use of the refined oral uptake description for D_4 to simulate the D_5 oral dosing study gave a similar overprediction of the peak rate of D_5 exhaled (data not shown). This indicated that D_5 was even more sequestered from exhalation with notable deviation in the first 12 h post dosing. As such, the uptake and tissue distribution parameters for the sequestered mass orally absorbed were adjusted to improve the simulation during the 1st 12 h post dosing. The model was able to capture this additional sequestration of D_5 from the oral dose after the 100 mg/kg oral bolus in rat. All of the data were well within a factor of three of the simulation for both parent D_5 (red lines and data) and total radioactivity (blue lines and data) with only the simulated 60 h rate of exhaled D5 being greater than a factor of two from the measured value (Fig. 8).

The revised MC-MD model was used to reproduce the human inhalation and dermal simulations reported in McMullin et al. (2016). Overall, the dermal simulations were little changed from that reported by McMullin for D_4 (Fig. 9) or D_5 (Fig. 10). This would indicate that scaling of deep compartment rate constants was appropriate. A comparison of potential plasma dose metrics for a bolus dose of D_4 (30 mg/kg) and D_5 (100 mg/kg) are shown in Table 4 where a 74 kg human and 0.2 kg rat are compared using the same dose as the rodent liquid diet dosing study. For D_4, while the maximum plasma concentration in human was approximately 30% greater than the rat, the plasma average concentration and $AUC_{(0–240\ h)}$ were nearly threefold higher. The predicted dose metrics for D5 in human; however, were similar to the rat for maximum concentration, $AUC_{(0–240\ h)}$ and average concentration.

4. Discussion

The MC-MD PBPK model for cyclic siloxanes reported by McMullin et al. (2016) was focused on bringing together the previously published models for D_4 and D_5 in rat and human in order to provide a unified code for siloxanes that could be used in human health risk assessment. In keeping with that theme, the focus of this effort was to incorporate the additional low dose oral time-course data after a single oral bolus in rodent liquid diet into the MC-MD model as earlier studies had questioned if the high bolus oral dose studies in rodents using various vehicles led to unusual absorption kinetics with the volatile cyclic siloxanes. The oral studies reported in Domoradzki et al. (2017) used a rodent liquid diet dosing solution and collected both plasma and tissue data for parent siloxane as had been reported for inhalation studies in rats. The addition of the tissue data allowed evaluation of uptake and distribution of the parent compound which was not possible with the total radioactivity kinetic data that had been reported for the previous oral dosing studies. The tissue data for parent siloxane showed rapid distribution to liver and fat as well as a lack of availability to be exhaled. As such, the initial absorbed mass from the GI tract appeared to be highly sequestered in the blood. This is not surprising as Dobrev et al. (2008) had reported limited exhalation into a closed chamber system after oral absorption. The description of oral absorption added to the MC-MD model was initially based on the Dobrev construct with modification of the oral uptake being necessary to capture the initial distribution to liver and fat based on the recently reported kinetic data from the low dose oral studies (Demoradzki et al., 2017).

As a further refinement to the MC-MD model, rate constants for tissue distribution and excretion which had been fit to specific kinetic data, require allometric scaling in order for the model to be incorporated into human health risk assessment. The model described in this effort, includes scaling for all rate constants in the model while maintaining essentially identical fits to the data in both rat (inhalation) and human (inhalation and dermal) as had been reported by McMullin et al. (2016). Previously, sex specific parameters for rat and human were necessary to capture the differences in kinetics. Now, differences seen in the kinetic data between the sexes (primarily due to differences

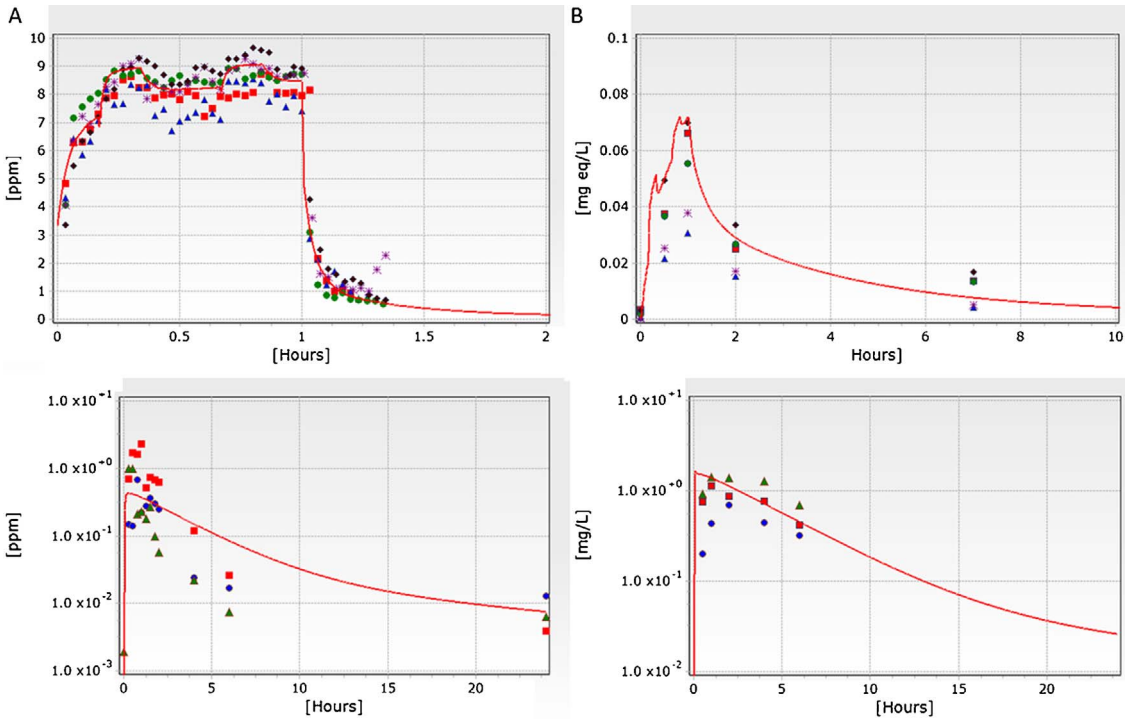

Fig. 10. Model simulation (lines) and data (symbols) (mean ± SD; $n = 3$) of D5 in (a) exhaled breath and (b) plasma in male human volunteers during and following 10 ppm D5 vapor exposure for 1-h (c) exhaled breath and (d) plasma during and following a single application of 1.4 g 13C-D5 to skin axilla.

Table 4
Comparison of rat to human plasma metrics for D_4 (30 mg/kg) or D_5 (100 mg/kg) after a single oral bolus. Body weight used for rat was 0.2 kg and for human was 74 kg.

Species	Metric	Units	D_4	D_5
Rat	Cmax	mg/L	5.61	6.77
	$AUC_{(0–240\ h)}$	mg-h/L	299.3	1105
	Avg. Conc.	mg/L	1.25	4.60
Human	Cmax	mg/L	7.32	6.55
	$AUC_{(0–240\ h)}$	mg-h/L	697.1	1078
	Avg. Conc.	mg/L	2.91	4.49

in BW) are now accounted for with allometric scaling. The impact of this on confidence in the MC-MD model is significant, as this simplifies the process for assessing cross-species dosimetry. We have also included induction of hepatic metabolism for both D_4 and D_5 in rat and human simulations based on the reports that the induction is essentially the same as seen for phenobarbital, which is known to induce metabolism in rats and humans (McKim et al., 1998, 1999, 2001; Parkinson et al., 2004). While the inclusion of induction had little impact on D_5 simulations for rat at the inhalation concentrations reported here and would not alter kinetics at low dose exposures in humans from consumer product use or environmental exposure, there is potential for induction to impact cross-species derivation of a risk metric (i.e., human equivalent concentration at a rat point of departure) that may require simulation of rat and human exposure scenarios higher than those from the human kinetic studies and higher than expected human consumer product or environmental exposures. Simulation of the low oral bolus dose used to refine the rat model with the human model, shows that the human is within a factor of 2 for D_4 and on par with the rat for D_5 (i.e., closer on a mg/kg basis than would be expected using body surface area interspecies scaling).

The unique nature of the volatile cyclic siloxanes (i.e., highly volatile and highly lipophilic) allow for better understanding of what is meant by “free” concentration in plasma for lipophilic chemicals. While the pseudo-physiological oral absorption description presented here has provided very good agreement with time-course oral bolus data for D4 and D5 in rat, the exact mechanism of this sequestered absorption is still uncertain. The model description may be refined further by studies that inform the distribution of the volatile cyclic siloxanes in plasma Future efforts with the MC-MD PBPK model will include incorporation of higher molecular weight siloxanes as well as further refinement of the metabolite submodels. It is possible that the less volatile nature of these siloxanes will be more amenable to addressing the distribution of the compounds in the plasma allowing further refinement of the MC-MD PBPK model.

The additional refinements to the MC-MD PBPK model presented here were initiated to provide a model that could serve as the basis for animal to human extrapolation across all potential dose routes (i.e., inhalation, dermal and oral) for human exposure. In addressing the rodent liquid diet oral bolus data and refining the model parameterization to include allometric scaling of all kinetic parameters, the D_4/D_5 MC-MD PBPK model can be incorporated into uncertainty and variability analysis which would not have been possible with any of the previously published cyclic siloxane models.

Conflicts of interest

None declared.

Transparency document

The http://dx.doi.org/10.1016/j.toxlet.2017.04.002 associated with this article can be found in the online version.

Acknowledgements

This work was supported by the Global Silicones Industry (GSC/SEHSC).

References

Andersen, M.E., Sarangapani, R., Reitz, R.H., Gallavan, R.H., Dobrev, I.D., Plotzke, K.P.,

2001. Physiological modeling reveals novel pharmacokinetic behavior for inhaled octamethylcyclotetrasiloxane in rats. Toxicol. Sci. 60, 214–231.
Brown, R.P., Delp, M.D., Lindstedt, S.L., Rhomberg, L.R., Beliles, R.P., 1997. Physiological parameter values for physiologically based pharmacokinetic models. Toxicol. Ind. Health 13 (4), 407–484.
Dobrev, I.D., Nong, A., Liao, K.H., Reddy, M.B., Plotzke, K.P., Andersen, M.E., 2008. Assessing kinetic determinants for metabolism and oral uptake of octamethylcyclotetrasiloxane (D4) from inhalation chamber studies. Inhal Toxicol. 20, 361–373.
Domoradzki, J.Y., Sushynski, C., McNett, D.A., Van Landingham, C., Plotzke, K.P., 2017. Metabolism and disposition of. (in preparation).
McKim Jr., J.M., Wilga, P.C., Kolesar, G.B., Choudhuri, S., Madan, A., Dochterman, L.W., Breen, J.G., Parkinson, A., Mast, R.W., Meeks, R.G., 1998. Evaluation of octamethylcyclotetrasiloxane (D_4) as an inducer of rat hepatic microsomal cytochrome P450, UDP-glucuronosyltransferase, and epoxide hydrolase: a 28-day inhalation study. Toxicol. Sci. 41 (1), 29–41.
McKim Jr., J.M., Choudhuri, S., Wilga, P.C., Madan, A., Burns-Naas, L.A., Gallavan, R.H., Mast, R.W., Naas, D.J., Parkinson, A., Meeks, R.G., 1999. Induction of hepatic xenobiotic metabolizing enzymes in female Fischer-344 rats following repeated inhalation exposure to decamethylcyclopentasiloxane (D_5). Toxicol. Sci. 50 (1), 10–19.
McKim Jr., J.M., Kolesar, G.B., Jean, P.A., Meeker, L.S., Wilga, P.C., Schoonhoven, R., Swenberg, J.A., Goodman, J.I., Gallavan, R.H., Meeks, R.G., 2001. Repeated inhalation exposure to octamethylcyclotetrasiloxane produces hepatomegaly, transient hepatic hyperplasia, and sustained hypertrophy in female Fischer 344 rats in a manner similar to phenobarbital. Toxicol. Appl. Pharmacol. 172 (2), 83–92.
McMullin, T.S., Yang, Y., Campbell, J., Clewell, H.J., Plotzke, K., Andersen, M.E., 2016. Development of an integrated multi-species and multi-dose route PBPK model for volatile methyl siloxanes – D_4 and D_5. Regul. Toxicol. Pharmacol. 74 (Suppl), S1–S13.
Parkinson, A., Mudra, D.R., Johnson, C., Dwyer, A., Carroll, K.M., 2004. The effects of gender, age, ethnicity, and liver cirrhosis on cytochrome P450 enzyme activity in human liver microsomes and inducibility in cultured human hepatocytes. Toxicol. Appl. Pharmacol. 199 (3), 193–209.
Plotzke, K.P., Crofoot, S.D., Ferdinandi, E.S., Beattie, J.G., Reitz, R.H., Mcnett, D.A., Meeks, R.G., 2000a. Disposition of radioactivity in Fischer 344 rats after single and multiple Inhalation Exposure to [(14)C]Octamethylcyclotetrasiloxane ([(14) C]D(4)). Drug Metab. Dispos. 28 (2), 192–204.
Plotzke, K.P., Utell, M.J., Looney, J.R., 2000b. Absorption, Distribution and Elimination of 13C-D4 in Humans after Dermal Administration. EPA document. 86010000007.
Plotzke, K.P., Utell, M.J., Looney, J.R., 2002. Absorption, Distribution and Elimination of 13C-D5 in Humans after Dermal Administration. EPA document. 84030000008.
Reddy, M.B., Andersen, M.E., Morrow, P.E., Dobrev, I.D., Varaprath, S., Plotzke, K.P., Utell, M.J., 2003. Physiological modeling of inhalation kinetics of octamethylcyclotetrasiloxane in humans during rest and exercise. Toxicol. Sci. 72, 3–18.
Reddy, M.B., Looney, R.J., Utell, M.J., Plotzke, K.P., Andersen, M.E., 2007. Modeling of human dermal absorption of octamethylcyclotetrasiloxane (D_4) and decamethylcyclopentasiloxane (D_5). Toxicol. Sci. 99, 422–431.
Reddy, M.B., Dobrev, I.D., Mcnett, D.A., Tobin, J.M., Utell, M.J., Morrow, P.E., Domoradzki, J.Y., Plotzke, K.P., Andersen, M.E., 2008. Inhalation dosimetry modeling with inhaled decamethylcyclopentasiloxane in rats and humans. Toxicol. Sci. 105, 275–285.
Sarangapani, R., Teeguarden, J., Andersen, M.E., Reitz, R.H., Plotzke, K.P., 2003. Route-specific differences in distribution characteristics of octamethylcyclotetrasiloxane (D_4) in rats: analysis using PBPK models. Toxicol. Sci. 71, 41–52.
Tobin, J.M., Mcnett, D.A., Durham, J.A., Plotzke, K.P., 2008. Disposition of decamethylcyclopentasiloxane in Fischer 344 rats following single or repeated inhalation exposure to 14c-decamethylcyclopentasiloxane (14c-D_5). Inhal. Toxicol. 20, 513–531.
Utell, M.J., Gelein, R., Yu, C.P., Kenaga, C., Geigel, T.A., Chalupa, D., Gibb, F.R., Speers, D.M., Mast, R.W., Morrow, P.E., 1998. Quantitative exposure of humansto an octamethylcyclotetrasiloxane (D4) Vap. Toxicol. Sci. 44, 206–213.
Varaprath, S., Mcmahon, J.M., Plotzke, K.P., 2003. Metabolites of hexamethyldisiloxane and decamethylcyclopentasiloxane in Fischer 344 rat urine - a comparison of a linear and a cyclic siloxane. Drug Metab. Dispos. 31, 206–214.
Varaprath, S., Salyers, K.L., Plotzke, K.P., Nanavati, S., 1999. Identification of metabolites of octamethylcyclotetrasiloxane (D4) in rat urine. Am. Soc. Pharm. Exp. Ther. 27, 1267–1273.
Zhang, J., Falany, J.L., Xie, X., Falany, C.N., 2000. Induction of rat hepatic drug metabolizing enzymes by dimethylcyclosiloxanes. Chem. Biol. Interact. 124 (2), 133–147.